

# Stable classical structures in dissipative quantum chaotic systems

Lisandro A. Raviola,<sup>1</sup> Gabriel G. Carlo,<sup>1</sup> and Alejandro M. F. Rivas<sup>1,2</sup>

<sup>1</sup>*Departamento de Física, CNEA, Av. Libertador 8250, (C1429BNP) Buenos Aires, Argentina*

<sup>2</sup>*Instituto de Ciencias, Universidad Nacional de General Sarmiento,*

*J.M. Gutierrez 1150, (B1613GSX) Los Polvorines, Buenos Aires, Argentina*

(Dated: July 2, 2018)

We study the stability of classical structures in chaotic systems when a dissipative quantum evolution takes place. We consider a paradigmatic model, the quantum baker map in contact with a heat bath at finite temperature. We analyze the behavior of the purity, fidelity and Husimi distributions corresponding to initial states localized on short periodic orbits (scar functions) and map eigenstates. Scar functions, that have a fundamental role in the semiclassical description of chaotic systems, emerge as very robust against environmental perturbations. This is confirmed by the study of other states localized on classical structures. Also, purity and fidelity show a complementary behavior as decoherence measures.

PACS numbers: 03.65.Yz, 03.65.Sq, 05.45.Mt

Since the origin of quantum theory until present the correspondence between the classical and quantum views of nature has been a major source of debate. Two broad areas of physics have converged naturally towards its study. On one hand we have the semiclassical theory of closed systems, where the problem consists of linking the Hamiltonian with the unitary quantum evolution as  $\hbar \rightarrow 0$ . For integrable systems the EBK quantization scheme [1] provides a precise correspondence between quantum numbers and energy levels and between eigenfunctions and invariant tori. For chaotic systems the correspondence is not so precise but the Gutzwiller trace formula [2] and more recently, the short periodic orbits theory [3] are resources at our disposal. However, a complete description of chaotic eigenfunctions in terms of classical invariants is still lacking. On the other hand, we have the decoherence theory that has established a correspondence between dissipative quantum systems and their classical analogs [4]. These studies have enormous relevance nowadays not only from the theoretical, but also from the experimental point of view. In fact, decoherence poses an unavoidable difficulty to the coherent manipulation of small scale systems, which in addition generally have a complex dynamics. Hence quantum mechanics, nonlinear dynamics and decoherence are necessary ingredients in many areas of physics, involved in a broad range of theoretical models and implementations. Just a few examples are transport in cold atoms and BECs [5], nanodevices [6], microlasers [7, 8, 9], quantum dots [10], and chaotic scattering [11].

In view of this we can ask ourselves, are there any classical structures embedded in the quantum realm that emerge as specially resistant to external perturbations? If so, in which way? To answer this questions, in this letter we investigate the stability of initial states with different degrees of classical information under the effects of chaotic evolution and decoherence. The environment is introduced by coupling the system to a heat bath at

finite temperature, in a way close to actual experimental situations. In order to capture all the essential features of dissipative quantum chaotic systems without unnecessary complications, we focus our study on dissipative quantum maps [12]. They constitute an ideal testbed for semiclassical and decoherence theories.

We find that scar functions, which are states localized along the stable and unstable manifolds of periodic orbits, are highly stable with respect to environmental perturbations. We quantify this stability by studying the purity and the fidelity, quantities that show complementary in order to measure decoherence. Moreover, by analyzing the Husimi distributions in phase space we conclusively show this behavior.

We perform the evolution of the density matrix of the system by means of a two step operator  $\rho$  [12, 13]. We use a composition of a unitary step given by the closed map  $B$  (representing the system dynamics), and a purely dissipative step given by the superoperator  $\mathbf{D}_\alpha$ , in the form

$$\rho' = \mathbf{S}(\rho) = \mathbf{D}_\alpha(\mathbf{B}(\rho)) \quad (1)$$

In this equation  $\mathbf{B}$  represents the unitary superoperator and  $\alpha$  all the parameters of the environmental model. In the following we explain the construction of these two steps.

We consider the baker map  $\mathcal{B}$  on the unit torus [14] as the system. It is given by  $(q', p') = \mathcal{B}(q, p) = (2q - [2q], p + [2q]/2)$  where  $(q, p)$  are the position and momentum coordinates and  $[x]$  stands for the integer part of  $x$ . This transformation is an area-preserving, uniformly hyperbolic, piecewise-linear and invertible map with Lyapunov exponent  $\lambda = \ln 2$ . The phase space has a very simple Markov partition consisting of two regions ( $q < 1/2$  and  $q \geq 1/2$ ) associated with the symbols 0 and 1, for which there is a complete symbolic dynamics. The action of the map upon symbols can be understood by means of the binary expansion of the coordinates

$(p|q) = \dots \nu_{-1} \cdot \nu_0 \nu_1 \dots \xrightarrow{\mathcal{B}} (p'|q') = \dots \nu_{-1} \nu_0 \cdot \nu_1 \dots$  where  $q = \sum_{i=0}^{\infty} \nu_i 2^{-(i+1)}$  and  $p = \sum_{i=-1}^{-\infty} \nu_i 2^i$ . Then, a periodic orbit (PO) of period  $L$  can be represented by a binary string  $\nu$  of length  $L$ . The coordinates of the first trajectory point  $(q_0, p_0)$  on the periodic orbit can be obtained explicitly in terms of the binary string as  $q_0 = \cdot \nu \nu \nu \dots = \nu / (2^L - 1)$  and  $p_0 = \cdot \nu^\dagger \nu^\dagger \nu^\dagger \dots = \nu^\dagger / (2^L - 1)$ , where  $\nu$  is the integer value of the string  $\nu$  which represents a binary number, and  $\nu^\dagger$  is the string formed by all  $L$  bits of  $\nu$  in reverse order. The other trajectory points can be easily calculated by iterations of the map or by cyclic shifts of  $\nu$ .

When quantizing this system any state  $|\psi\rangle$  must satisfy periodic boundary conditions on the torus, for both the position and momentum representations. This amounts to taking  $\langle q+1|\psi\rangle = e^{i2\pi\chi_q} \langle q|\psi\rangle$ , and  $\langle p+1|\psi\rangle = e^{i2\pi\chi_p} \langle p|\psi\rangle$ , with  $\chi_q, \chi_p \in [0, 1)$ . This implies a Hilbert space of finite dimension  $N = (2\pi\hbar)^{-1}$ . The discrete set of position and momentum eigenstates is given by  $|q_j\rangle = |(j + \chi_q)/N\rangle$  ( $j = 0, 1, \dots, N-1$ ), and  $|p_k\rangle = |(k + \chi_p)/N\rangle$  ( $k = 0, 1, \dots, N-1$ ), labeled by the corresponding eigenvalues  $q_j, p_k$ . They are related by a discrete Fourier transform, i.e.  $\langle p_k|q_j\rangle = 1/\sqrt{N} \exp(-i(2\pi/N)(j + \chi_q)(k + \chi_p)) \equiv (G_N^{\chi_q, \chi_p})$ . Throughout the paper we assume a phase space with anti-symmetric boundary conditions ( $\chi_q = \chi_p = 1/2$ ). The unitary operator  $\hat{B}$  that performs the closed quantum evolution is given by [14, 15]:

$$\hat{B} = G_N^\dagger \begin{pmatrix} G_{N/2} & 0 \\ 0 & G_{N/2} \end{pmatrix}. \quad (2)$$

We incorporate dissipation and thermalization to the quantum map by coupling it to a bath of noninteracting oscillators in thermal equilibrium at a temperature  $T$ . The degrees of freedom of the bath can be eliminated by means of the usual weak coupling, Markov and rotating wave approximations [16]. As a result we arrive at a Lindblad equation for the density matrix of the system  $\rho$  that can be written as a completely positive map  $\mathbf{D}_\alpha(dt)$  in the operator-sum (or Kraus) representation

$$\rho(t+dt) = \mathbf{D}_{(\varepsilon, T)}(dt)(\rho(t)) = \sum_{\mu=0}^2 K_\mu \rho(t) K_\mu^\dagger \quad (3)$$

where

$$\begin{aligned} K_0 &= \mathbb{1} - \frac{1}{2} \sum_{\mu=1}^2 K_\mu^\dagger K_\mu \\ K_1 &= \sum_{k=1}^{N-1} \sqrt{\varepsilon dt (1 + \bar{n}(k)) k} |p_{k-1}\rangle \langle p_k| \\ K_2 &= \sum_{k=1}^{N-1} \sqrt{\varepsilon dt \bar{n}(k) k} |p_k\rangle \langle p_{k-1}| \end{aligned} \quad (4)$$

are the infinitesimal Kraus operators satisfying  $\sum_\mu K_\mu^\dagger K_\mu = \mathbb{1}$  to first order in  $dt$  [17]. In these equations  $\varepsilon$  is a system-bath coupling parameter that can be associated to a classical velocity dependent damping (at  $T = 0$  gives the contraction rate of the phase space). The population densities of the bath are given by  $\bar{n} = (\exp(\Delta E_k / (k_B T)) - 1)^{-1}$ , where we have taken  $E_k = p_k^2/2$ , and the Boltzmann constant  $k_B = 1$ . Then, we integrate  $\mathbf{D}_{(\varepsilon, T)}(dt)$  numerically to obtain the dissipative step.

We now briefly describe the scar function construction [18, 19, 20], the main tools we use to study the stability of classical structures. These functions are also essential in the semiclassical description of chaotic eigenfunctions [3]. They are wavefunctions highly localized on the stable and unstable manifolds of POs, and on the energy given by a Bohr-Sommerfeld quantization condition on the trajectory. We are going to use a formulation suitable for maps on the torus, though they apply also to general flows. The first step is to define the *Periodic Orbit Modes* (POMs) for maps,  $|\phi_{\text{POM}}^{\text{maps}}\rangle$  as a sum of coherent states centered at the fixed points of a given PO  $\nu$ , each one having a phase [20] (see Figure 3(a) for an example). Then, the scar function is obtained after applying a dynamical average and can be written as

$$|\phi_{\text{scar}}^{\text{maps}}\rangle = \sum_{l=-T}^T e^{iS_\nu l/\hbar} \cos\left(\frac{\pi l}{2T}\right) B^l |\phi_{\text{POM}}^{\text{maps}}\rangle, \quad (5)$$

where  $T$  stands for the number of iterations of the map up to the Ehrenfest time  $T_E = \ln N/\lambda$ , and  $S_\nu$  is the classical action of  $\nu$  (see Figure 3(b) for an example). It is worth mentioning that for  $T = 0$  the POMs are recovered, but as  $T$  is increased this function sharpens its quasi-energy width while extending in phase space along the stable and unstable manifolds of the periodic orbit. Eventually, it turns into a true eigenstate if the propagation time reaches the order of the Heisenberg time.

In our calculations we have considered five types of initial states. Besides the already mentioned scar states and POMs, we have studied the behavior of eigenstates of the map having a significant overlap with scar functions. Also, we have considered states developed along the stable and unstable manifolds. These last two cases correspond to eigenstates of the momentum and position operators, since for the baker map the direction of the manifolds coincide with those of the corresponding axes. In addition, we have selected  $q$  and  $p$  values that represent points belonging to the periodic orbits shown. In summary, we compare states with relevant classical imprints (localized on POs and their manifolds) with strictly quantum states (map eigenstates). All results correspond to  $N = 100$ .

The behavior of the coherence is studied through the purity, defined as  $P = \text{tr}(\rho^2)$  (tr denotes the trace). We find that the scar functions, the map eigenstates that

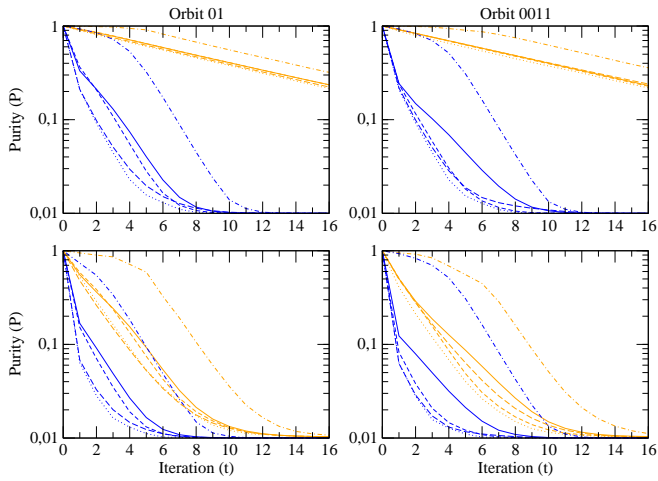


Figure 1: (Color online) Purity  $P$  (logarithmic scale) as a function of time (measured in units of map steps). In the left column we show results for the orbit  $\nu = 01$ , while in the right one for  $\nu = 0011$ . Upper panels correspond to  $\varepsilon = 0.001$ , and lower ones to  $\varepsilon = 0.01$ . Orange (lighter) lines correspond to  $T = 1$  and blue (darker) lines to  $T = 1000$ . Solid lines stand for scar functions, long-dashed lines for eigenstates of the map, short-dashed for POMs, dot-dashed for position eigenstates and dotted for momentum eigenstates.  $N = 100$ .

have a maximum overlap with them, and the POMs, all behave in a similar way. However, the purity decay is faster in the case of the eigenstates when compared to that of the corresponding scar functions. On the other hand the position eigenstates are the less and the momentum eigenstates the most decoherent ones. We show results for two representative orbits in the left and right columns of Figure 1 (they are denoted by  $\nu = 01$  and  $\nu = 0011$ , respectively). In obtaining these results we have considered two different couplings with the environment ( $\varepsilon = 0.001$  and  $\varepsilon = 0.01$ ), and two different values of the temperature ( $T = 1$  and  $T = 1000$ ). They convalidate the hypothesis that entropy production, then entanglement with the environment, is governed by the classical unstable behavior of the system [4]. The more localized on classically unstable regions the initial distribution is, the fastest its entropy production results.

In order to have a complementary stability criterion we have explored the fidelity calculated as  $F = \sqrt{\langle \psi | \rho | \psi \rangle}$ . This quantity measures the degree of overlap between the pure initial state  $|\psi\rangle$  and the evolved density matrix  $\rho$ . This time we find that although the scar functions and the corresponding map eigenstates have a similar behavior, the latter are more stable than the former when the temperature is low. For higher values the situation changes and the scar functions become more stable than the eigenfunctions. The coupling with the environment seems to play a similar role than temperature, since the decay rate difference for low values of  $T$  shrinks as  $\varepsilon$  grows. Finally, POMs fidelity decays faster, and the po-

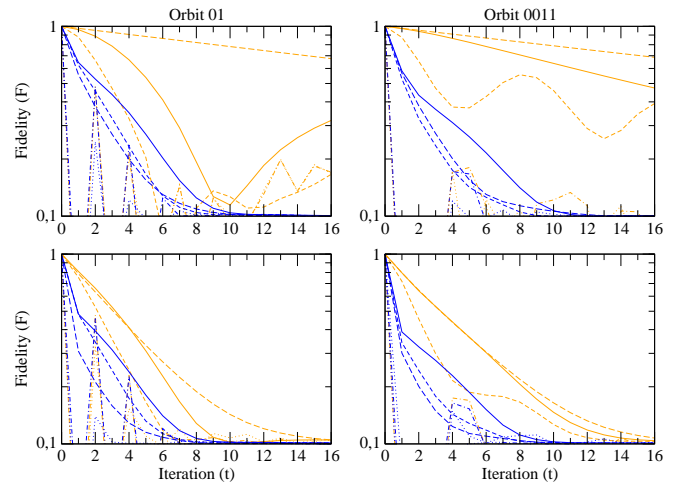


Figure 2: Fidelity  $F$  (logarithmic scale) as a function of time (measured in units of map steps). We show results for the same orbits, use the same parameter values, and colors and patterns criterion as in Fig. 1.

sition and momentum eigenstates have the greatest decay rate but with big oscillations, whose periodicity is given by the dynamics. Hence, for low temperatures the stability is governed by the quantum mechanics of the system. Initial states that are closer (greater overlap) to the map eigenfunctions turn out to be the most stable ones. In this sense, scar functions are more stable than POMs, which in turn are more stable than position and momentum eigenstates. When the effects of the environment become stronger scar functions emerge again as remarkably stable, having the lowest decay rate of all the initial states we have considered. This is shown in Fig. 2, where we have used the same orbits, parameter values, colors and patterns as those chosen for Fig. 1.

The picture is completed by means of the Husimi distributions obtained at different times. They can be seen in Figure 3, where the evolution of the POMs, the scar functions and the map eigenstates for the orbit  $\nu = 0011$  can be found. The high stability of the scar functions is undoubtedly demonstrated. When already the POMs shape cannot be distinguished anymore they still display a high level of detail, showing their characteristic localization along the manifolds of the corresponding orbit. Moreover, the eigenstate rapidly loses its original details and seems to converge to the scar function.

In conclusion, we have verified a great degree of complementarity between purity and fidelity as decoherence measures. The loss of purity, or entropy production, is governed by the classical instability of the system, while the fidelity decay for low temperatures (and weak coupling with the bath) is dominated by the overlap of the initial state with the map eigenfunctions. When temperature rises the situation changes and the localization on classical structures plays again a fundamental

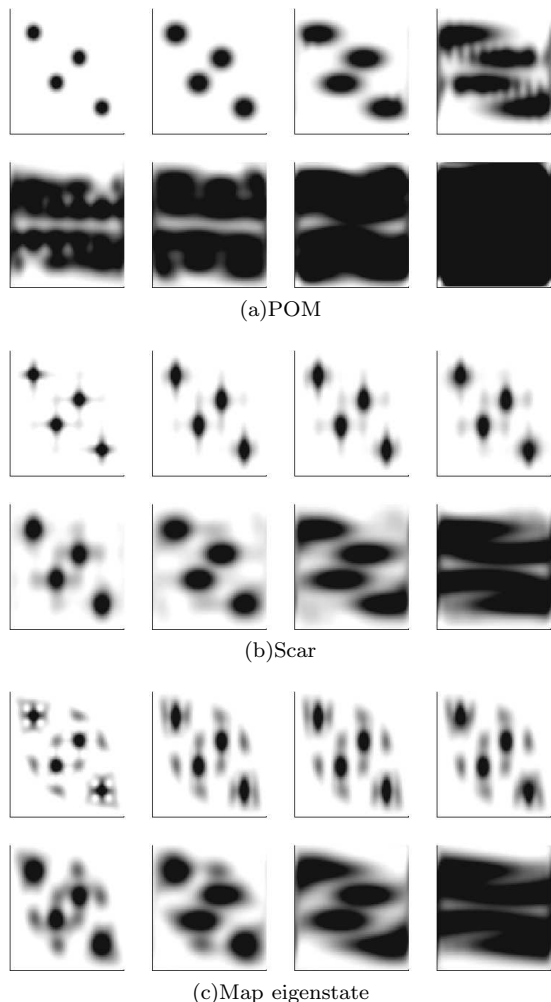


Figure 3: Husimi distributions for the POM and scar function associated to orbit  $\nu = 0011$  ((a) upper and (b) middle panels, respectively), and corresponding map eigenstate ((c) lower panel). We have used  $\varepsilon = 0.01$  and  $T = 1000$ . Time steps go from 0 to 7 from left to right and top to bottom. The grayscale goes from white (minimum probability) to black (maximum probability).

role. By analyzing these quantities we have found classical structures in quantum mechanics that are specially stable when subjected to environmental perturbations. They are the scar functions, which are associated to periodic orbits and the stable and unstable manifolds in their vicinity. Husimi distributions in phase space allowed us to clarify this picture. We have conclusively shown that scar functions keep their shape virtually intact at times when the POMs have already lost all their characteristic features. Hence, more than just localization on the periodic points is needed to provide stability. Finally, by exploiting the simplicity of the manifolds of our map we could verify that any kind of localization on them is not enough to guarantee robustness against external pertur-

bations, but the one provided by scar functions.

Remarkably, the purity and fidelity loss of the map eigenstates (in this last case with the exception of low temperatures) is generally faster than that of the scar functions. Then, these latter represent the stable classical skeleton of the map eigenstates against environmental perturbations. It is worth underlining that these classical structures which survive for longer times are also the main classical ingredient needed to construct the eigenstates, according to the short periodic orbit theory.

Support by CONICET is gratefully acknowledged.

- 
- [1] M. Brack and R.K. Bhaduri, *Semiclassical Physics*, Addison-Wesley, Reading MA (1997).
  - [2] M.C. Gutzwiller, *Chaos in Classical and Quantum Mechanics*, Springer, New York (1990).
  - [3] E. Vergini, J. Phys. A **33**, 4709 (2000); E. Vergini and G.G. Carlo, J. Phys. A **33**, 4717 (2000); E. Vergini, D.M. Schneider, A.M.F. Rivas, J. Phys. A **41**, 405102 (2008).
  - [4] W.H. Zurek, Rev. Mod. Phys. **75**, 715 (2003); W.H. Zurek and J.P. Paz, Phys. Rev. Lett. **72**, 2508 (1994); D. Monteoliva and J.P. Paz **85**, 3373 (2000).
  - [5] C. Mennerat-Robilliard *et al.*, Phys. Rev. Lett. **82**, 851 (1999); P.H. Jones *et al.*, Phys. Rev. Lett. **98** 073002 (2007); M. Sadgrove, M. Horikoshi, T. Sekimura, and K. Nakagawa, Phys. Rev. Lett. **99**, 043002 (2007); I. Dana, V. Ramareddy, I. Talukdar, and G.S. Summy, Phys. Rev. Lett. **100**, 024103 (2008).
  - [6] R.D. Astumian, Science **276**, 917 (1997).
  - [7] W. Fang, Phys. Rev. A **72**, 023815 (2005); J.U. Nöckel and D.A. Stone, Nature (London) **385**, 45 (1997); T. Harayama, P. Davis and K.S. Ikeda, Phys. Rev. Lett. **90**, 063901 (2003);
  - [8] J. Wiersig and M. Hentschel, Phys. Rev. A **73** 031802(R) (2006); Phys. Rev. Lett. **100**, 033901 (2008).
  - [9] J. Wiersig, Phys. Rev. Lett. **97** 253901 (2006).
  - [10] R. Akis *et al.*, Phys. Rev. Lett. **79**, 123 (1997).
  - [11] P. Gaspard, *Chaos, Scattering and Statistical Mechanics*, Cambridge Univ. Press, Cambridge (1998); C. Jung and T.H. Seligman, Phys. Rep. **285**, 77 (1997).
  - [12] P. Bianucci, J. P. Paz, and M. Saraceno, Phys. Rev. E **65**, 046226 (2002)
  - [13] I. García-Mata *et al.*, Phys. Rev. A **72**, 062315 (2005)
  - [14] N.L. Balazs and A. Voros, Ann. Phys. **190**, 1 (1989);
  - [15] M. Saraceno, Ann. Phys. **199**, 37 (1990).
  - [16] C. W. Gardiner and P. Zoller, *Quantum Noise* (Springer-Verlag, Berlin, 1991).
  - [17] G.G. Carlo, G. Benenti, G. Casati, C. Mejía-Monasterio, Phys. Rev. A **69**, 062317 (2004).
  - [18] G.G. de Polavieja, F. Borondo, and R.M. Benito, Phys. Rev. Lett. **73**, 1613 (1994).
  - [19] E.G. Vergini and G.G. Carlo, J. Phys. A **34**, 4525 (2001); E.G. Vergini and D. Schneider, J. Phys. A **38**, 587 (2005); A.M.F. Rivas, J. Phys A **40**, 11057 (2007).
  - [20] F. Faure, S. Nonnenmacher, and S. De Bievre, Commun. Math. Phys. **239**, 449 (2003).